Modeling a dielectric elastomer as driven by triboelectric nanogenerator

Xiangyu Chen, Tao Jiang, and Zhong Lin Wang

Citation: Appl. Phys. Lett. **110**, 033505 (2017); doi: 10.1063/1.4974143
View online: http://dx.doi.org/10.1063/1.4974143
View Table of Contents: http://aip.scitation.org/toc/apl/110/3
Published by the American Institute of Physics

Modeling a dielectric elastomer as driven by triboelectric nanogenerator

Xiangyu Chen,[1] Tao Jiang,[1] and Zhong Lin Wang[1,2,a)]
[1]*Beijing Institute of Nanoenergy and Nanosystems, Chinese Academy of Sciences, National Center for Nanoscience and Technology (NCNST), Beijing 100083, People's Republic of China*
[2]*School of Materials Science and Engineering, Georgia Institute of Technology, Atlanta, Georgia 30332-0245, USA*

(Received 17 October 2016; accepted 3 January 2017; published online 18 January 2017)

By integrating a triboelectric nanogenerator (TENG) and a thin film dielectric elastomer actuator (DEA), the DEA can be directly powered and controlled by the output of the TENG, which demonstrates a self-powered actuation system toward various practical applications in the fields of electronic skin and soft robotics. This paper describes a method to construct a physical model for this integrated TENG-DEA system on the basis of nonequilibrium thermodynamics and electrostatics induction theory. The model can precisely simulate the influences from both the viscoelasticity and current leakage to the output performance of the TENG, which can help us to better understand the interaction between TENG and DEA devices. Accordingly, the established electric field, the deformation strain of the DEA, and the output current from the TENG are systemically analyzed by using this model. A comparison between real measurements and simulation results confirms that the proposed model can predict the dynamic response of the DEA driven by contact-electrification and can also quantitatively analyze the relaxation of the tribo-induced strain due to the leakage behavior. Hence, the proposed model in this work could serve as a guidance for optimizing the devices in the future studies. *Published by AIP Publishing*. [http://dx.doi.org/10.1063/1.4974143]

The dielectric elastomer is a kind of stretchable material with a low elastic modulus and a large strain capability.[1–3] By sandwiching a dielectric elastomer film between two compliant electrodes, a simple actuator structure can be established. When a high voltage drop is applied on this dielectric elastomer actuator (DEA) sample, electrostatic attraction occurs between opposite charges on two electrodes and accordingly, the elastomer film reduces in thickness and expands in area. Based on this basic working principle, the DEA can be further developed as various smart electromechanical systems, such as braille displays, life-like robots, tunable lens, and power generators.[1–5] To operate a DEA, a dielectric elastomer is often subject to transient, time-dependent voltage signals and thus both displacement current and current leakage dominate the charge accumulation on the interface. Meanwhile, the dynamic performance of the DEA is also affected by the viscoelasticity of the elastomer.[6–8] Hence, in order to optimize the efficiency of the DEA, a detailed mechanism analysis with the consideration of both viscoelasticity and charge relaxation processes is quite necessary.

On the other hand, the self-powered nano-system is a recently emerged concept that can spare the external power supply by directly collecting energy from the ambient environment.[9–12] Meanwhile, the triboelectric nanogenerator (TENG) based on the conjunction of contact electrification and electrostatic induction effects has been demonstrated to be an excellent and universal energy harvester for most nano-systems.[12–15] A unique advantage of the TENG is that its output voltage is typically high even though its volume is rather small, which allows it to serve as a high voltage source to drive or control some electromechanical systems. The conjunction system of the TENG-DEA can fully utilize the advantages of both techniques and thus a series of interesting applications in the field of smart actuators and wearable electronics can be developed.[16,17] For this TENG-DEA conjunction system, although its basic function has been demonstrated, there still lacks a theoretical model to systematically provide an in-depth understanding of its working principle.

In this paper, a comprehensive theoretical model is developed for the TENG-DEA system. We systematically studied the real time output characteristics from the TENG and the related dynamic deformation strain of the DEA by utilizing numerical calculation methods. The viscoelasticity of the DEA is represented by a nonlinear spring-dashpot model and the leakage phenomenon of the elastomer is considered by using an empirical equation. The proposed model can precisely simulate the real-time interaction between the TENG and DEA, which provides us an in-depth physical picture about the operation of this integrated system. The analyzing method and the physical model proposed in this paper can serve as an important guidance for structure design of the device towards the optimum performance in various specific applications.

The structure of the integrated self-powered TENG-DEA system as well as the basic operation method for this system is illustrated in Figure 1(a). The sliding single-electrode mode TENG is chosen for establishing a simple analytical formula, while a similar analyzing method can be applied for other type TENG devices. The sliding single-electrode mode TENG is structurally composed of two plates (Figure 1(a)): the metal foil with a rectangular shape plays dual roles of a triboelectric surface and the output electrode; the dielectric film on the surface of the top sliding plate is

a)E-mail: zhong.wang@mse.gatech.edu

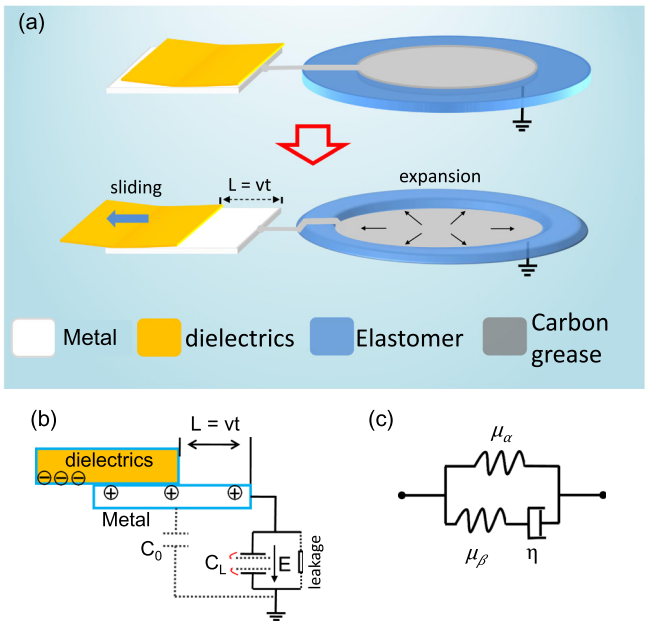

FIG. 1. (a) Sketch of a TENG-DEA system and the deformation behavior caused by sliding motion. (b) Theoretical model for the TENG-DEA system. (c) Theoretical model for viscoelasticity of the elastomer.

chosen as the other tribo-electric layer. When a dielectric film contacts with the metal foil, the positive and negative surface charges are induced on the surfaces of metal foil and dielectrics, respectively. The successive sliding motion results in a high potential drop established between metal foil and the ground, while this potential drop will be endured by the dielectric elastomer.

The theoretical model related to this TENG-DEA system can be found in Figure 1(b). An imaginary capacitor C_0 is placed between metal foil and the ground, which represents the ground capacitance of the TENG. This C_0 is a fixed value according to the working mechanism of the single-electrode TENG ($C_0 \ll C_L$).[16] The DEA is simply modelled as a capacitor (C_L). During the operation, the activated deformation of elastomer results in the change of the capacitance of C_L. In our case, the displacement current is related to the current arises with capacitors with dielectric medium between the electrodes. That is, the changing of the electric field and the changing of the capacitance can both lead to the motion of the charges, which can both induce the changing of the output current from the TENG. We need to consider the displacement current caused by this capacitance changing. Meanwhile, when the elastomer film is connected to a power source, a small current may flow through the film, which is known as current leakage. This leakage may depend on the molecular configuration, defects and impurities in the structure, which is very difficult to be modelled as analytical equations. The previous studies[6] suggested a model based on following empirical observations for analyzing this leakage phenomenon through the elastomer. The density of leakage current ($I_{leakage}$) can be related to the electric field (E) as: $I_{leakage} = \sigma_0 \exp(E/E_r)E$, where σ_0 is the basic conductivity at low field and E_r is an empirical constant. When $E \ll E_r$, the elastomer approximates an Ohmic conductor. When E is close to E_r, the conductivity increases exponentially. In this case, the output current (I_{TENG}) from the TENG to the DEA is given as

$$I_{TENG} = C_L(t)\frac{dV}{dt} + V\frac{dC_L(t)}{dt} + \sigma_0 \exp\left(\frac{E}{E_r}\right)E, \quad (1)$$

where V is the output voltage from the TENG.

The deformation of the elastomer is due to the existence of Maxwell stress caused by the electric field across the thickness direction.[1–3] The Maxwell stress (P) is generated from the electrostatic attraction between the charges on the opposing electrodes and it can be given as:[1–3] $P = -\varepsilon\varepsilon_0 E^2$, where ε is the permittivity of the elastomer layer. Hence, when the radius of the elastomer electrode increases from R to r, its thickness reduces from d to d'. In our analyses, we assume that the elastomer film experiences a homogeneous and equal-biaxial deformation and the elastomer is incompressible materials. Accordingly, if the stretch strain is defined as $\lambda = r/R$, the capacitance (C_L) of the elastomer under the deformation strain is $\lambda^4 C_L$, where C_L is the original capacitance without deformation. To analyze the viscoelastic relaxation of the DEA, we employ a well-established rheological model of springs and dashpots for elastomer film, as can be seen in Figure 1(c).[6–8] Two parallel units are adopted for the model, where one unit consists of a spring with the shear modulus μ_α and the other unit consists of a spring with the shear modulus μ_β and a dashpot with Newtonian fluid characteristics (the viscosity η) (Figure 1(c)). Here, the stretches of the dielectric elastomer film λ are assumed to be the net stretches of both units. The ξ is the stretches in the dashpot and the stretches of the spring β are $\lambda^\beta = \lambda\xi$. By employing the non-equilibrium thermodynamic theory and the neo-Hookean material model,[8,18] the viscoelasticity model of the dielectric elastomer under the stress ρ and the electric field E can be written as

$$\rho + \varepsilon\varepsilon_0 E^2 = \mu_\alpha(\lambda^2 - \lambda^{-4}) + \mu_\beta(\lambda^2\xi^{-2} - \xi^4\lambda^{-4}), \quad (2)$$

$$\frac{1}{\xi}\frac{d\xi}{dt} = \frac{1}{3\eta}\frac{\mu_\beta}{2}\left(\lambda^2\xi^{-2} - \xi^4\lambda^{-4}\right). \quad (3)$$

This kinetic model satisfies the thermodynamic inequality if $\eta > 0$. In this article, we focus on the viscoelastic relaxation of the dielectric elastomer under the drive of an electric field generated by the TENG. It is important to note that the analysis in this paper is based on the neo-Hookean material model, where the stiffening effect of the elastomeric films at large deformation is ignored. In order to address the stiffening effect of the elastomer, we can consider the Gent model in further investigations, as done by Suo *et al.*[6,7]

For the ideal case, the leakage current through the elastomer is neglected and the output voltage from the TENG as well as the established electric field across the DEA can be written as[20–23]

$$\begin{cases} 0 < t < L/v \\ V_{TENG}(t) = \dfrac{\sigma w v t}{C_0 + C_L\lambda(t)^4} \quad E_{TENG}(t) = \dfrac{\sigma w v t}{C_0 + C_L\lambda(t)^4}\dfrac{\lambda(t)^2}{d} \\ L/v < t \\ V_{TENG}(t) = \dfrac{\sigma w L}{C_0 + C_L\lambda(t)^4} \quad E_{TENG}(t) = \dfrac{\sigma w L}{C_0 + C_L\lambda(t)^4}\dfrac{\lambda(t)^2}{d}, \end{cases} \quad (4)$$

where v is the motion velocity, w is the width of the electrode, σ is the average surface charge density, L is the maximum motion distance, and d is the original thickness of the elastomer without deformation. On the other hand, if we consider the influence from the leakage current through the elastomer, Eq. (4) is deduced as

$$\begin{cases} 0 < t < L/v \\ V_{TENG}(t) = \dfrac{\sigma w v t - \int_0^t dQ_{leakage}}{C_0 + C_L \lambda(t)^4} \quad E_{TENG}(t) = \dfrac{\sigma w v t - \int_0^t dQ_{leakage}}{C_0 + C_L \lambda(t)^4} \dfrac{\lambda(t)^2}{d} \\ L/v < t \\ V_{TENG}(t) = \dfrac{\sigma w L - \int_0^t dQ_{leakage}}{C_0 + C_L \lambda(t)^4} \quad E_{TENG}(t) = \dfrac{\sigma w L - \int_0^t dQ_{leakage}}{C_0 + C_L \lambda(t)^4} \dfrac{\lambda(t)^2}{d}, \end{cases} \tag{5}$$

where $\int_0^t dQ_{leakage}$ is the charge leaked through the DEA. By combining Eqs. (2)–(5), the dynamic deformation of the DEA under the excitation of tribo-motion (L is the motion distance) can be written as a series of first-order ordinary differential equations, as can be seen in Eqs. (S1) and (S2) in the supplementary material. To simplify the analysis, we assume that at $t = 0$, $\lambda(0) = 1$, $\xi(0) = 1$, and output voltage from the TENG is $V(0) = 0$. By choosing a proper time step Δt, the stretches in the spring (λ) and in dashpot (ξ) at the next time step $t_1 = t_0 + \Delta t$ can be obtained from the first-order ordinary differential equations (supplementary material Eqs. (S1) and (S2)) by using the improved Euler method.[19] Meanwhile, the related capacitance of the elastomer and the output voltage from the TENG at the same time can also be determined accordingly. Thereafter, by continuously repeating this calculation with the increase of time, all the parameters within a continuous time domain can be determined step by step.

In order to clarify the influence of the elastomer deformation on the output performance of the single-electrode TENG, we first analyze the physical model without the leakage current (Eqs. (2)–(4)). It is important to note that the influence from the leakage phenomenon is so significant that it may overlap the contribution from the viscoelasticity relaxation. Hence, it is necessary to consider the ideal case without leakage, only to highlight the contribution of the viscoelasticity of the film. The detailed calculation parameters are listed in Table S1 (supplementary material), while the results can be found in Figures 2(a)–2(d). Figure 2(a) shows the deformation strain of the DEA under the excitation of the TENG under different motion speeds. The motion distance in Figure 2(a) is 10 cm. Hence, in the ideal case, the strain is determined by the accumulated charges on the DEA (namely, the motion distance) and the motion speed can only decide the relaxation time of the DEA. The established electric field across DEA is also calculated as shown in Figure 2(b). In the high speed case (0.1 m/s), when the motion of the TENG is stopped, the expansion of the DEA is not over yet. Hence, the electric field exhibits a sharp peak after the motion stops (see Figure 2(b)). In Figure 2(c), the motion speed is fixed to be 0.01 m/s, while the motion distance varies from 10 cm to 30 cm. The saturated strain of the DEA is increased with the increase of the motion distance, which confirms that the extent of the strain is mostly determined by the motion distance. The output current from the TENG is also calculated by using Eq. (1), as can be seen in Figure 2(d). When the motion is stopped, the output current still flows for a period after that, which is caused by the displacement current related to the capacitance changing of the elastomer ($V\frac{dC_L(t)}{dt}$).

The deformation of the DEA without considering the leakage phenomenon is an ideal case for the DEA. In order to get a whole physical picture of the TENG-DEA system, we must include the leakage current in our model. Based on Eqs. (2), (3), and (5), we analyze the physical model with the leakage current, and the deformation strain actuated by the contact-electrification is calculated in Figures 3(a)–3(d), where three different basic conductivities of the leakage phenomenon ($\sigma_0 = 3 \times 10^{-16}$–$7 \times 10^{-16}$ S/m) are designed for revealing the influence of the leakage current. As can be seen in Figures 3(a)–3(d), for the same leakage current, the

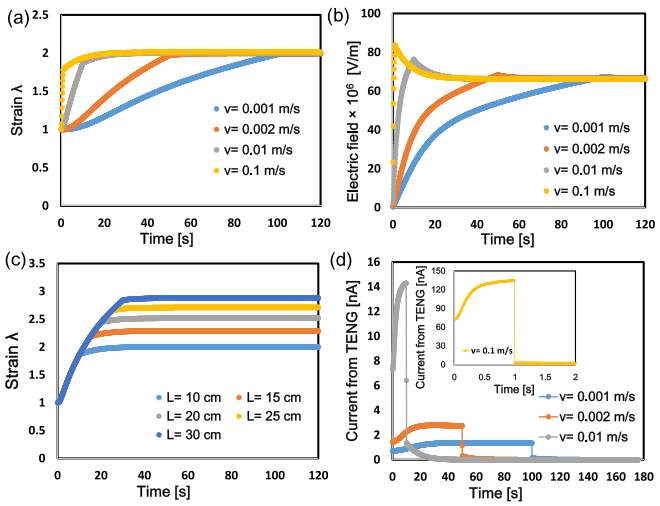

FIG. 2. Simulation of the operation of the TENG-DEA system without the consideration of the leakage phenomenon. (a) The actuated strain with different motion speeds, while the motion distance is fixed to be 10 cm. (b) The established electric field across the DEA device with different motion speeds. (c) The actuated strain with different motion distances, while the motion speed is 0.01 m/s. (d) The output current from the TENG with different motion speeds.

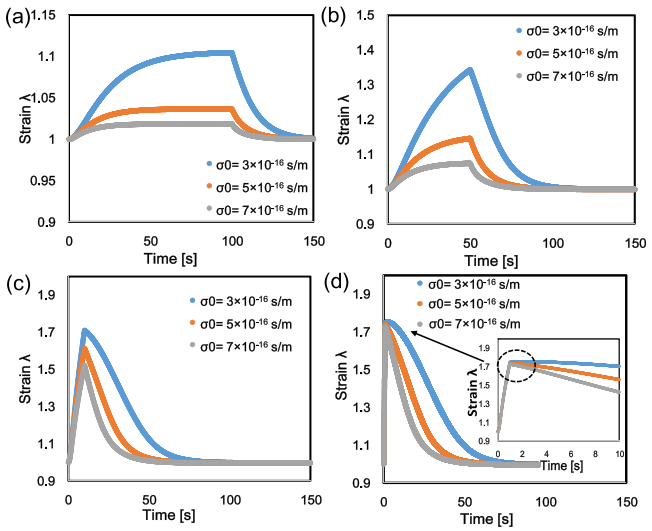

FIG. 3. Simulation of the actuated strain of the TENG-DEA system with the consideration of the leakage phenomenon, where the basic conductivity σ_0 changes from 3×10^{-16} to 7×10^{-16} S/m. (a) The motion speed is 0.001 m/s. (b) The motion speed is 0.002 m/s. (c) The motion speed is 0.01 m/s. (d) The motion speed is 0.1 m/s.

higher motion speed can generate higher deformation strain. Meanwhile, the TENG-DEA system can show almost the same maximum strain with the common motion speed (0.1 m/s–0.01 m/s), which proved the application compatibility of this TENG-DEA for human-machine interaction. Only if the motion speed is extremely slow (0.001 m/s), the actuated strain will be significantly suppressed, which is due to the continuous contribution from leakage current. On the other hand, as can be seen in Figure 3(a), even though the maximum strain for speed of 0.001 m/s is quite small, this strain value can be maintained for a rather long time (until the motion stops). Hence, if the charge generation rate can well match the leakage current, a stable actuated strain can be achieved without attenuation, which offers a possibility to use this TENG-DEA system as artificial muscle to stably manipulate or hold some objects.

As can be seen in Figures 3(a)–3(d), the coordination between the charge generation rate and the leakage current value can significantly influence the performance of the DEA. Hence, we perform a detailed calculation of the leakage current and the total output current for different motion speeds, as shown in Figures S1(a)–S1(h) (supplementary material). For the low speed case (0.001 m/s and 0.002 m/s), the total output current from the TENG is almost the same as the leakage current (see Figures S4(a)–S4(d), supplementary material), which suggests that the leakage phenomenon dominates the charge transfer process. For the time period from 50 s to 100 s, the leakage current is equal to the total output current and the displacement current is close to zero, indicating that the charge generation rate can well match the leakage current. For the motion speed of 0.01 m/s, the total output current from the TENG starts to be larger than leakage current (see Figures S1(e) and S1(f), supplementary material). As for the motion speed of 0.1 m/s, the leakage current is less than one third of the total output current (see Figures 4(g) and 4(h)). As shown in Figure S1, by increasing the motion speed, the influence of the leakage current can be suppressed, which is helpful for achieving a higher maximum strain. However, the existence of the leakage phenomenon can seriously harm the stability of the strain, which is one of the most crucial problems needed to be solved for the real application of this TENG-DEA system. As can be seen in Figure 3, the increase of the basic conductivity for the leakage model significantly weakens the maximum value and the persistence of the actuated strain. We also performed some further calculation related to this point, as can be seen in Figure S2. The further increase of the conductivity (10 times greater) results in the decrease of the maximum strain and the fast relaxation of the actuated strain. Meanwhile, if we increase the motion velocity to be 0.5 m/s, the maximum strain can be compensated, while the relaxation process of the strain after stopping the motion still cannot be improved. It is thus quite necessary to develop some surface modification methods to block the leakage current or to synthesize some advanced elastomer materials with lower conductivity.

The deformation performance of the TENG-DEA system was measured experimentally, in order to demonstrate the validity of the theoretical analysis. The Al foil and Kapton dielectric film are applied for the sliding single-electrode TENG (see Figure 1(a)), while the commercial Acrylic elastomers (0.25 mm thick, VHB 9473, 3M) without any pre-strain are applied for the DEA. The persistence of the actuated strain within 2 min after tribo-electrification has been measured experimentally and been simulated based on the proposed physical model, as shown in Figure 4(a). The motion speed is 0.1 m/s and the motion distance is 10 cm. The simulation results are in good agreement with the experimental data. The fitting parameters for the viscoelastic and leakage model are also listed in Figure 4(a). The variation of

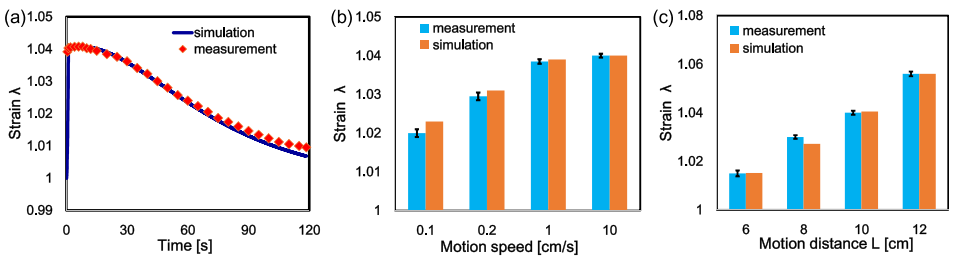

FIG. 4. (a) The relaxation process of the actuated strain, where the dotted line is the experimental data and the solid line is the simulation results. The motion distance is 10 cm and the velocity is 0.1 m/s. (b) The induced strain of the DEA with different motion velocities of the TENG and the comparison between experimental data and simulations, where the motion distance is 10 cm. (c) The measurements and the simulation of actuated strain with different motion distances, where the motion speed is 0.1 m/s.

the parameter is due to the detailed operation condition of the elastomer sample and this will not influence the validity of our model. It is important to note that these basic parameters are not changed for a specified sample. Hence, the same sample under various driving motions (speed, motion distance, and so on) can be predicted by the theoretical model. Based on a similar theoretical model and the same TENG-DEA sample, the contribution of the motion speed to the maximum strain is also studied and tested experimentally, as can be seen in Figure 4(b). The measurements are all performed for more than 5 times and the generated error bars are also shown in Figure 4(b). The changing tendency of the simulation results and the real data are in good agreement with each other. However, we also found that the decrease of the strain for the low speed case is more significant than the simulation results, which can be attributed to the more serious leakage phenomenon in the real measurements (may be due to the influence of the free ions in the air). In order to better simulate these processes, a modified leakage model is necessary in the future study. The actuated strains with different motion distances are also studied based on this model, as can be seen in Figure 4(c). The simulation results are comparable with the real measurements. Hence, the comparison between the simulations and the real measurements confirms the validity of the physical model. The interaction between the leakage effect and the output from the TENG can be precisely simulated by using the proposed analyzing method, and the detailed deformation performance of the TENG-DEA system can also be qualitatively predicted by this model.

In summary, the equivalent circuit model and the integrated simulation for the TENG-DEA system are proposed by coupling nonequilibrium thermodynamics and electrostatic induction theory. The influences from both the viscoelasticity and current leakage to the output performance of the TENG are systematically analyzed and the real-time simulations of the actuated strain under various motion speeds are carried out for the DEA. Under the same motion distance, the maximum strain increases with the increase of motion speed. Meanwhile, a stable strain can be maintained with the low speed, if the charge generation rate can well match the leakage current. It is hoped that the proposed physical model can serve as an aid to better explore the practical applications of this integrated system in the field of electronic skin or some other soft electronic devices.

See supplementary material for the designed parameters in the simulation and the current output from the TENG to the DEA.

This work was supported by the National Key R&D Project from Minister of Science and Technology (2016YFA0202704), the "thousands talents" program for pioneer researcher and his innovation team, China, and National Natural Science Foundation of China (Grant Nos. 61405131, 51432005, 5151101243, 51561145021, and 11374204).

[1]F. Carpi, S. Bauer, and D. D. Rossi, Science **330**, 1759–1761 (2010).
[2]S. Shian, K. Bertoldi, and D. R. Clarke, Adv. Mater. **27**, 6814–6819 (2015).
[3]C. H. Yang, B. Chen, J. Zhou, Y. M. Chen, and Z. Suo, Adv. Mater. **28**, 4480–4484 (2016).
[4]F. Carpi, G. Frediani, M. Nanni, and D. D. Rossi, IEEE/ASME Trans. Mechatronics **16**, 16–23 (2011).
[5]T. McKay, B. O'Brien, E. Calius, and I. Anderson, Smart Mater. Struct. **19**, 055025 (2010).
[6]C. C. Foo, S. Cai, S. Koh, S. Bauer, and Z. Suo, J. Appl. Phys. **111**, 034102 (2012).
[7]J. Huang, T. Li, C. Chiang Foo, J. Zhu, D. R. Clarke, and Z. Suo, Appl. Phys. Lett. **100**, 041911 (2012).
[8]H. Wang, M. Lei, and S. Cai, J. Appl. Phys. **113**, 213508 (2013).
[9]S. Xu, Y. Qin, C. Xu, Y. G. Wei, R. S. Yang, and Z. L. Wang, Nat. Nanotechnol. **5**, 366–373 (2010).
[10]M. D. Han, X. S. Zhang, B. Meng, W. Liu, W. Tang, X. Sun, M. W. Wang, and H. X. Zhang, ACS Nano **7**, 8554–8560 (2013).
[11]G. T. Hwang, H. Park, J. H. Lee, S. Oh, K. I. Park, M. Byun, H. Park, G. Ahn, C. K. Jeong, K. No, H. Kwon, S. G. Lee, B. Joung, and K. J. Lee, Adv. Mater. **26**, 4880–4887 (2014).
[12]J. H. Lee, K. Y. Lee, M. K. Gupta, T. Y. Kim, D. Y. Lee, J. Oh, C. Ryu, W. J. Yoo, C. Y. Kang, S. J. Yoon, J. B. Yoo, and S. W. Kim, Adv. Mater. **26**, 765–769 (2014).
[13]Q. Liang, X. Yan, X. Liao, S. Cao, X. Zheng, H. Si, S. Lu, and Y. Zhang, Nano Energy **16**, 329–338 (2015).
[14]J. Zhong, Y. Zhang, Q. Z. Zhong, Q. Y. Hu, B. Hu, Z. L. Wang, and J. Zhou, ACS Nano **8**, 6273–6280 (2014).
[15]X. Chen, M. Iwamoto, Z. Shi, L. Zhang, and Z. L. Wang, Adv. Funct. Mater. **25**, 739–747 (2015).
[16]X. Chen, T. Jiang, Y. Yao, L. Xu, Z. Zhao, and Z. L. Wang, Adv. Funct. Mater. **26**, 4906–4913 (2016).
[17]X. Chen, X. Pu, T. Jiang, A. Yu, L. Xu, and Z. L. Wang, "Tunable optical modulator by coupling a triboelectric nanogenerator and a dielectric elastomer," Adv. Funct. Mater. **27**, 1603788 (2017).
[18]X. H. Zhao, S. Koh, and Z. Suo, Int. J. Appl. Mech. **3**, 203–217 (2011).
[19]X. Chen, T. Jiang, Z. Sun, and W. Ou-Yang, Appl. Phys. Lett. **107**, 114103 (2015).
[20]S. M. Niu, Y. Liu, S. H. Wang, L. Lin, Y. S. Zhou, Y. F. Hu, and Z. L. Wang, Adv. Funct. Mater. **24**, 3332–3340 (2014).
[21]T. Jiang, X. Chen, C. B. Han, W. Tang, and Z. L. Wang, Adv. Funct. Mater. **25**, 2928–2938 (2015).
[22]T. Jiang, X. Chen, K. Yang, C. B. Han, W. Tang, and Z. L. Wang, Nano Res. **9**, 1057–1070 (2016).
[23]X. Chen, D. Taguchi, T. Manaka, M. Iwamoto, and Z. L. Wang, Sci. Rep. **5**, 13019 (2015).